Scintillation quenching by Ir^{3+} impurity in cerium doped lutetium pyrosilicate crystals

Scintillation quenching by Ir^{3+} impurity in cerium doped lutetium pyrosilicate crystals

L Pidol[1,2]**, O Guillot-Noël**[1]**, M Jourdier**[1]**, A Kahn-Harari**[1]**, B Ferrand**[3]**, P Dorenbos**[4] **and D Gourier**[1]

[1] Ecole Nationale Supérieure de Chimie de Paris (ENSCP), Laboratoire de Chimie Appliquée de l'Etat Solide, UMR-CNRS 7574, 11 rue Pierre et Marie Curie, 75231 Paris Cedex 05, France
[2] Saint Gobain Cristaux et Détecteurs, 104 route de Larchant, 77140 Saint Pierre les Nemours, France
[3] LETI/DOPT/STCO/Laboratoire Cristallogenèse Appliquée—CEA Grenoble, 17 rue des Martyrs, 38054 Grenoble Cedex 09, France
[4] Radiation Technology Group, Interfaculty Reactor Institute, Delft University of Technology, Mekelweg 15, 2629 JB Delft, The Netherlands

E-mail: didier-gourier@enscp.jussieu.fr

Abstract
Cerium doped lutetium pyrosilicate $Lu_2Si_2O_7:Ce^{3+}$ (LPS) single crystals, prepared by the floating zone technique, present good scintillation properties, with a light yield between 15 000 and 31 000 photons MeV^{-1}. However, some LPS crystals prepared by the Czochralski process exhibited quite a low scintillation light output, below 2000 photons MeV^{-1}. Electron paramagnetic resonance experiments show that this scintillation quenching is due to iridium impurities (Ir^{3+}) originating from the iridium crucible.

1. Introduction

The development of cerium doped lutetium oxides, such as LSO ($Lu_2SiO_5:Ce$) [1] and LuAP ($LuAlO_3:Ce$) [2, 3] is motivated by the need for an improved scintillator crystal for positron emission tomography (PET). These materials exhibit the expected requirements for gamma detection scintillators, i.e. high density and high effective atomic number [4], high scintillation light yield and very short decay time. In particular, this is the case for the recently discovered cerium doped lutetium pyrosilicate $Lu_2Si_2O_7:Ce^{3+}$ (LPS) crystals [5, 6]. The light yield of single crystals synthesized by the melting zone technique always lies in the range 15 000–31 000 photons MeV^{-1} under γ-ray excitation and the cerium scintillation decay time is around 37 ns, with no observable afterglow [7]. However, there is a lack of light yield reproducibility for the LPS:Ce^{3+} crystals grown by the Czochralski process. Some of them display a high light output, about 26 000 photons MeV^{-1}, as reported in [6], whereas for others the light yield was found to be lower than 2000 photons MeV^{-1}. Since the cerium energy level

structure does not allow any significant intrinsic quenching mechanism, some impurities or defects could be at the origin of this light yield quenching. Electron paramagnetic resonance (EPR) spectroscopy is a powerful tool to identify and characterize the various defects created by irradiation in scintillator materials [8–11]. The EPR study of several crystals before and after irradiation points out Ir^{3+} impurities as a quencher of the scintillation light output.

2. Materials and experimental methods

LPS crystals were grown by the floating zone technique or by a vertical pulling method, the Czochralski technique, with iridium crucibles. Light yields at 662 keV (γ-rays from ^{137}Cs) were measured with a Hamamatsu R1791 photomultiplier tube (PMT), as described elsewhere [12]. The samples studied by EPR were x-ray oriented and cut in specific crystallographic directions. EPR measurements were performed at 15 K, using a Bruker ESP 300E X-band spectrometer. All irradiations were done at room temperature, using an x-ray tube with a Cu anode operating at 35 kV and 25 mA for 2 h or a γ-ray source ^{137}Cs (662 keV) for 30 min. After irradiation and before the EPR experiments, the crystals were kept in a dark environment. EPR simulations were performed with the program SimFonia (WinEPR, Version 1.0) from Bruker. Thirteen LPS samples were studied in this work. They are divided into three sets:

  (i) group A: LPS:Ce^{3+} samples grown by the floating zone technique,
 (ii) group B: LPS:Ce^{3+} samples grown by the Czochralski method and which present a low light output, and
(iii) group C: LPS:Ce^{3+} samples grown by the floating zone technique and intentionally co-doped with iridium.

3. Results and discussion

The main characteristics of the LPS samples, including the crystal growth techniques, the initial concentrations of doping ions, EPR and light yield results are gathered in table 1. The largest light yields are observed for crystals grown by the melting zone technique (group A) with values ranging from 15 000 to 31 000 photons MeV^{-1}. In contrast, the photon yields of LPS crystals grown by the Czochralski method and presented here (group B) are very low, less than 2000 photons MeV^{-1}.

Before irradiation, no significant differences are observed in the EPR spectra of the crystals coming from groups A and B. These EPR spectra are shown in figure 1 for samples LPS A_1 and LPS B_1, respectively, recorded with the magnetic field perpendicular to the *c*-axis. At 15 K, the intense EPR line is due to Ce^{3+} ions with *g*-factor values $g_x = 2.992$, $g_y = 0.689$ and $g_z = 0$. This signal is not observed in undoped samples (spectrum not presented here). The free Ce^{3+} ion has a $4f^1$ configuration with a $^{2S+1}L_J = {}^2F_{5/2}$ ground state, where S, L and J are the spin, orbital and total momenta, respectively. In the LPS structure, Ce^{3+} ions substitute Lu^{3+} ions in a site of very low symmetry. The ground state $^2F_{5/2}$ splits into three Kramers doublets, $|M_J| = 5/2$, $3/2$ and $1/2$, in a low crystal field, M_J being the *z*-component of J. As only the lowest doublet is populated at liquid helium temperature, and as cerium has no isotope with non-zero nuclear spin, the EPR spectrum can be described by an effective spin $S = 1/2$ and the EPR spectrum of Ce^{3+} is expected to be composed of a single intense line as seen in figure 1. Upon increasing the temperature, this line disappears around 100 K, because of the lifetime broadening of the EPR line resulting from the decrease of the spin–lattice relaxation time of Ce^{3+} ion.
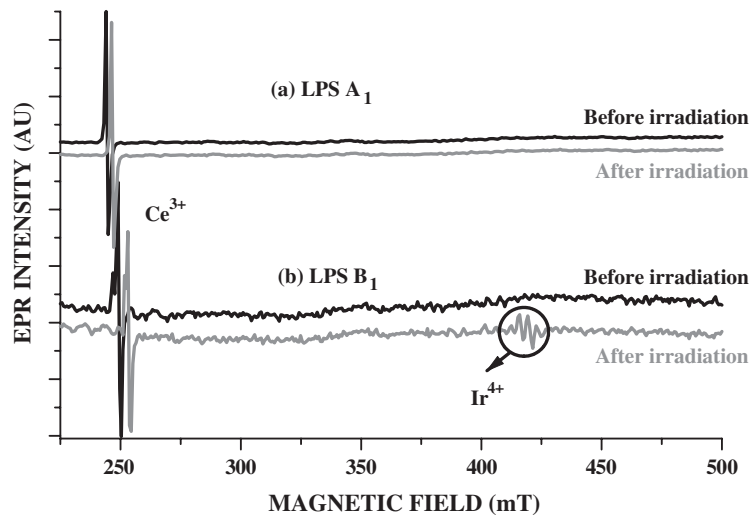
Figure 1. EPR spectra at 15 K of LPS A_1 and B_1 before and after x-ray irradiation. LPS A_1 sample, grown by the floating zone method, presents good scintillation properties (27 000 photons MeV^{-1}). LPS B_1 sample, grown by the Czochralski process (from an iridium crucible), shows a very low scintillation light output (700 photons MeV^{-1}). The spectra were recorded at 9.5 GHz with a microwave power of 20 mW, and modulation amplitude 1 mT. The magnetic field is parallel to the $a * b$ plane, at 68° from the b-axis.

Table 1. Main characteristics of LPS crystals.

| Samples	Crystal growth	Initial concentration of doping ions	Light yield (photons MeV^{-1})[a]	Irradiation	Ir^{4+} EPR signal
LPS A_1	Melting zone	0.5% Ce	27 000	X and γ	No
LPS A_2		0.5% Ce	16 900	X and γ	No
LPS A_3		0.5% Ce	21 600	X	No
LPS A_4		0.5% Ce	31 000	X	No
LPS A_6		0.5% Ce	29 800	X	No
LPS A_7		0.5% Ce	21 400	X	No
LPS B_1	Czochralski	0.5% Ce	700	X and γ	Yes
LPS B_2	(Iridium crucible)	0.5% Ce	<2 000	X and γ	Yes
LPS B_3		0.5% Ce	<2 000	X	Yes
LPS B_4		0.05% Ce	<2 000	X	Yes
LPS B_5		0.05% Ce	<2 000	X	Yes
LPS C_1	Melting zone	0.5% Ce + 0.1% Ir	1 500	X and γ	Yes
LPS C_2		0.5% Ce + 0.1% Ir	5 000	X	Yes

[a] Source: ^{137}Cs (662 keV), shaping time: 10 μs, PMT: Hamamatsu R1791, errors in the yield: around 10%.

After x-ray or γ-ray irradiation, all LPS samples with a low light output (group B) exhibit an additional EPR signal around 350–410 mT, as shown in figure 1 for sample B_1. The structure and the position of this signal depend on the crystal orientation. This additional signal never occurs for crystals presenting good light yields (group A, figure 1). As this signal is not seen with non-irradiated samples, it can be linked to a diamagnetic defect which becomes

paramagnetic under irradiation. This defect could be an impurity ion, such as a transition-metal ion (partially filled nd shell) or rare-earth ion (partially filled 4f shell), which can change its valence state under irradiation [8–10, 13–18].

The EPR signal induced by irradiation is relatively complicated. However, along some specific orientations of the crystal in the magnetic field, four lines are observed (figure 1(b)). This multiplet structure is attributed to the hyperfine interaction between an electron spin $S = 1/2$ and a nuclear spin $I = 3/2$. The g-values, deduced from the EPR signal upon rotating the sample in the magnetic field, are $g_x = 1.715$, $g_y = 1.779$ and $g_z = 1.962$, with the g_z tensor axis parallel to the crystallographic axis c. The four lines are not exactly equally spaced, probably due to a second order effect of the hyperfine interaction and/or a quadrupole interaction. In a first approximation, the average hyperfine interaction $\langle A \rangle = 1/3(A_x+A_y+A_z)$ can be evaluated around 25×10^{-4} cm^{-1} (2.9 mT). In some specific orientations, each of the four lines splits into two other lines, revealing two sets of four lines. Due to a strong linewidth anisotropy, only an average hyperfine pattern of four lines is observed, for some orientations. Therefore, this signal likely arises from a metallic ion having two isotopes with nuclear spin $I = 3/2$. Only iridium and copper correspond to this situation. Indeed, Cu^{2+} ion ($3d^9$) has two isotopes, ^{63}Cu and ^{65}Cu, with nuclear spins $I = 3/2$ and with a natural abundance of 69.2% and 30.8%, respectively. However, for this ion, the g-factor values are usually higher than the free electron value, $g_e = 2.0023$ [19]. Iridium has two isotopes, ^{191}Ir and ^{193}Ir, with nuclear spins $I = 3/2$ and a natural abundance of 37.3% and 62.7%, respectively. The two paramagnetic valence states of iridium, $Ir^{2+}(5d^7)$ and $Ir^{4+}(5d^5)$, may have low spin configuration with an electron spin $S = 1/2$. Furthermore, the presence of an iridium impurity could be easily explained by a contamination from the iridium crucibles. To confirm this hypothesis, crystals intentionally co-doped with cerium and iridium were synthesized by the melting zone technique (group C). These crystals present a very low light yield, lower than 5000 photons MeV^{-1} (table 1). No EPR signal which could be associated to iridium is detected in the as-grown LPS crystals before irradiation, which indicates that iridium enters in the LPS matrix with the diamagnetic $5d^6$ Ir^{3+} state. An EPR signal, identical with that of figure 1, is observed after γ- or x-ray irradiation (see figure 2).

The attribution of the irradiation-induced defect to paramagnetic iridium ions is confirmed by simulating the four-line spectrum (figure 3). We have selected a specific orientation for LPS C_1, where the magnetic field is parallel to g_z and to the c-axis. The simulation is the sum of spectra for each iridium isotope, weighted by their natural abundance. The line-shape of transitions is Gaussian and the g_z-value is equal to 1.962. Assuming the presence of iridium impurities, we have taken the hyperfine splittings $^{193}A_z$ and $^{191}A_z$ equal to 28.2×10^{-4} and 25.7×10^{-4} cm^{-1} respectively (3.1 and 2.8 mT), according to the g_n ratio of the both isotopes ($^{193}g_n = 0.107$ and $^{191}g_n = 0.097$). Despite the fact that the spectrum exhibits a broad resonance line, the satisfying agreement between the simulation and the experimental spectra shows that this four-line pattern is compatible with the presence of two iridium isotopes and confirms, if necessary, that the additional signal is due to iridium ions. The last issue to be addressed is the exact oxidation state of the paramagnetic iridium ions, as both Ir^{2+} and Ir^{4+} are paramagnetic. Figure 4 presents the average hyperfine splitting, $\langle A \rangle$, as a function of the average g-value $\langle g \rangle = 1/3(g_x + g_y + g_z)$, for several compounds which contain Ir^{2+} ions [13–15, 18] or Ir^{4+} ions [16, 17, 20–25]. All the experimental points are clearly localized in well separated areas for these two ions. It clearly comes out that the values $\langle A \rangle = 25 \times 10^{-4}$ cm^{-1} (2.9 mT) and $\langle g \rangle = 1.819$ of the irradiation-induced defect in LPS correspond to the Ir^{4+} ion. It thus appears likely that iridium ions coming from the iridium crucible enter into the crystal structure during the crystal growth by the Czochralski method. This has already been mentioned in other works [22, 23]. Iridium impurities in the diamagnetic state $Ir^{3+}(5d^6)$ occupy
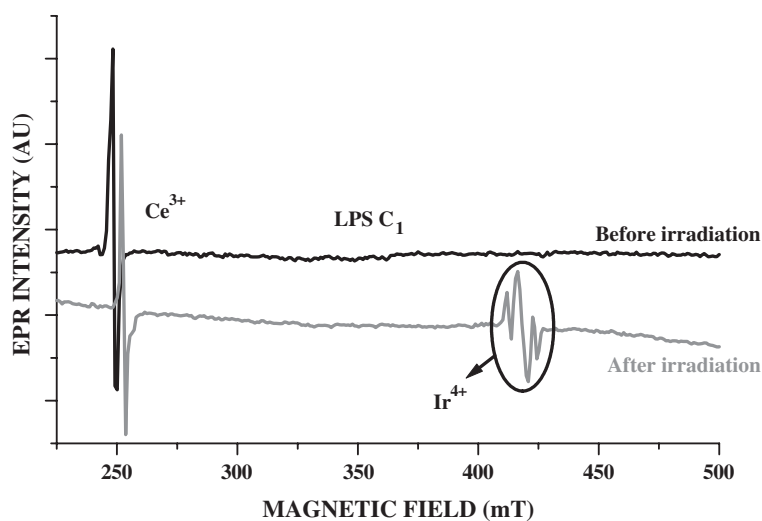
Figure 2. EPR spectra at 15 K of LPS C_1 before and after x-ray irradiation. This crystal, grown by the floating zone technique, was intentionally doped with 0.1% of IrO_2. The spectra were recorded at 9.5 GHz with a microwave power of 20 mW, and modulation amplitude 1 mT. The magnetic field is parallel to the $a * b$ plane, at 68° from the b-axis.
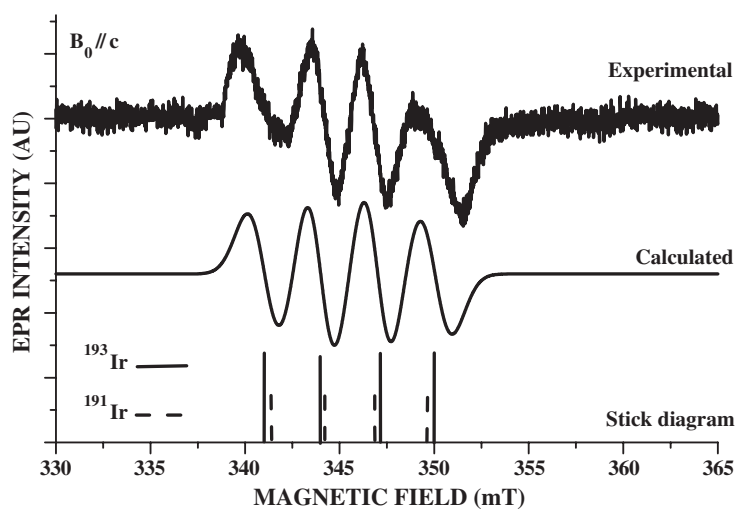

Figure 3. Zoom on the additional EPR signal observed after x-ray irradiation in LPS C_1, for B_0 parallel to the c-axis. The spectra were recorded at 9.5 GHz with a microwave power of 20 mW, and modulation amplitude 0.3 mT. Simulation parameters: $g_z = 1.962$, $^{193}A_z = 28.2 \times 10^{-4}$ cm^{-1} (3.1 mT), $^{191}A_z = 25.7 \times 10^{-4}$ cm^{-1} (2.8 mT), Gaussian line-shape, linewidth $\Delta B = 1.55$ mT.

Lu^{3+} sites of the structure and form a localized state below the Fermi level in the forbidden gap of LPS. Thus, irradiations induce the formation of Ir^{4+} by hole (h^+) trapping:

$$Ir^{3+} + h^+ \rightarrow Ir^{4+}.$$
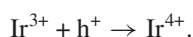
This reaction is reversible by heating or by a long exposure to daylight, as the additional EPR signal disappears. The very good correlation between the presence of iridium impurities and
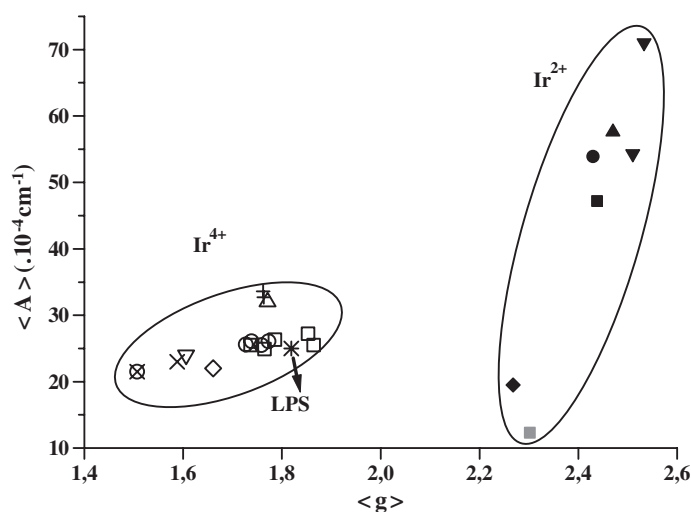
Figure 4. Comparison of the average *g*-value $\langle g \rangle$ and the average hyperfine interaction $\langle A \rangle$ of the irradiation-induced EPR signal in some LPS crystals (∗) to the values for several compounds containing Ir^{2+} or Ir^{4+} ions. ■ $CaO:Ir^{2+}$ and ▪ $MgO:Ir^{2+}$ [13], ● $AgCl:Ir^{2+}$ and ▲ $AgBr:Ir^{2+}$ [14], ▼ $NaCl:Ir^{2+}$ [15], ♦ $Ir(CN)_4Cl_2$ in NaCl [18]. ○ $CaO:Ir^{4+}$ and $MgO:Ir^{4+}$ [16], × $BaTiO_3:Ir^{4+}$ [17], □ $(IrX_6)^{2-}$ with $X^- = Cl^-$, Br^- or F^- [20], △ $Y_3Ga_5O_{12}:Ir^{4+}$ [21], ▽ $SrTiO_3:Ir^{4+}$ [22], ◇ $KNbO_3:Ir^{4+}$ [23], + $Cs_2HfCl_6:Ir^{4+}$ and $Cs_2ZrCl_6:Ir^{4+}$ [24], ⊗ $TiO_2:Ir^{4+}$ [25]. For this latter host, $\langle A \rangle$ is the average of A_x and A_y due to a lack of information.

the alteration of the scintillation yield conclusively shows that Ir^{3+} ions are responsible for the quenching.

4. Conclusion

Whereas $LPS:Ce^{3+}$ crystals grown by the melting zone technique always display a very high light output (from 15 000 to 31 000 photons MeV^{-1}), the $LPS:Ce^{3+}$ crystals grown by the Czochralski process present a lack of light yield reproducibility. Some Czochralski crystals exhibit very promising scintillation properties, with a high light output (about 26 000 photons MeV^{-1}), as reported in [6]. However, some crystals grown by the same process display a very low light yield (<5000 photons MeV^{-1}), which results from the presence of iridium impurities coming from the iridium crucible used for the Czochralski technique. This behaviour is correlated to the presence of an additional EPR signal produced by γ- or x-ray irradiation, for all crystals that show a low light output. This paramagnetic defect has been unambiguously assigned to Ir^{4+} ions. During the crystal growth, iridium enters into the crystals as Ir^{3+} ion and irradiation induces a change of valence state into Ir^{4+} ion by hole trapping. EPR, thermoluminescence and optical studies of these samples are in progress to further investigate the quenching mechanism of the scintillation properties.

Following this study, the crystal growth conditions have been improved leading to LPS crystals with good quality and reproducible scintillation behaviour [6].

Acknowledgments

References

[1] Melcher C L and Schweitzer J S 1992 *IEEE Trans. Nucl. Sci.* **39** 502
[2] Moses W W, Derenzo S E, Fyodorov A, Korzhik M, Gektin A, Minkov B and Aslanov V 1995 *IEEE Trans. Nucl. Sci.* **42** 275
[3] Lempicki A, Randles M H, Wisniewski D, Balcerzyk M, Brecher C and Wojtowicz A J 1995 *IEEE Trans. Nucl. Sci.* **42** 280
[4] van Eijk C W E 2001 *Nucl. Instrum. Methods* A **460** 1
[5] Pauwels D, Viana B, Kahn-Harari A, Dorenbos P and van Eijk C W E 2002 *US Patent Specification* 6437336
[6] Pidol L, Kahn-Harari A, Viana B, Ferrand B, Dorenbos P, de Haas J T M, van Eijk C W E and Virey E 2003 *J. Phys.: Condens. Matter* **15** 2091
[7] Pauwels D, Lemasson N, Viana B, Kahn-Harari A, van Loef E V D, Dorenbos P and van Eijk C W E 2000 *IEEE Trans. Nucl. Sci.* **47** 1787
[8] Zaldo C and Moya E 1993 *J. Phys.: Condens. Matter* **5** 4935
[9] Halliburton L E and Edwards G J 1994 *Mater. Res. Soc. Symp. Proc.* **348** 423
[10] Ferraz G M, Matsuoka M, Watanabe S and Sunta C M 1998 *Radiat. Eff. Defects Solids* **146** 303
[11] Schweizer S and Spaeth J M 1999 *J. Phys.: Condens. Matter* **11** 1723
[12] Dorenbos P, de Haas J T M, Visser R, van Eijk C W E and Hollander R W 1993 *IEEE Trans. Nucl. Sci.* **40** 424
[13] Raizman A, Suss J T and Low W 1975 *Phys. Rev.* B **15** 5184
[14] Eachus R S and Graves R E 1976 *J. Chem. Phys.* **65** 1530
[15] Vugman N V and Pinhal N M 1979 *Mol. Phys.* **38** 1999
[16] Raizman A and Suss J T 1980 *Phys. Rev.* B **22** 1141
[17] Possenriede E, Jacobs P and Schirmer O F 1992 *J. Phys.: Condens. Matter* **4** 4719
[18] Pinhal N M and Vugman N V 1985 *J. Phys. C: Solid State Phys.* **18** 6273
[19] Wertz J E and Bolton J R 1972 *Electron Spin Resonance, Elementary Theory and Practical Applications* (New York: McGraw Hill)
[20] Thornley J H M 1968 *J. Phys. C: Solid State Phys.* **1** 1024
[21] Andlauer B, Schneider J and Tolksdorf W 1976 *Phys. Status Solidi* b **73** 533
[22] Schirmer O F, Förster A, Hesse H, Wöhlecke M and Kapphan S 1984 *J. Phys. C: Solid State Phys.* **17** 1321
[23] Possenriede E, Schirmer O F, Donnerberg H J and Hellermann B 1989 *J. Phys.: Condens. Matter* **1** 7267
[24] Maniv S and Gabay A 1974 *J. Magn. Reson.* **13** 148
[25] Blazey K W and Levy F 1986 *Solid State Commun.* **59** 335